Remote Sensing of Environment 246 (2020) 111873

Contents lists available at ScienceDirect

Remote Sensing of Environment

journal homepage: www.elsevier.com/locate/rse

Monitoring cropland abandonment with Landsat time series

He Yin[a,*], Amintas Brandão Jr[b], Johanna Buchner[a], David Helmers[a], Benjamin G. Iuliano[c], Niwaeli E. Kimambo[a,d], Katarzyna E. Lewińska[a], Elena Razenkova[a], Afag Rizayeva[a], Natalia Rogova[a], Seth A. Spawn[b,d], Yanhua Xie[b], Volker C. Radeloff[a]

[a] SILVIS Lab, Department of Forest and Wildlife Ecology, University of Wisconsin-Madison, 1630 Linden Drive, Madison, WI 53706, USA
[b] Center for Sustainability and the Global Environment (SAGE), Nelson Institute of Environmental Studies, University of Wisconsin-Madison, 1710 University Avenue, Madison, WI 53726, USA
[c] Department of Integrative Biology, University of Wisconsin-Madison, 250 N Mills St, Madison, WI 53706, USA
[d] Department of Geography, University of Wisconsin-Madison, 550 N Park St, Madison, WI, 53706, USA

ARTICLE INFO

Keywords:
Agriculture
Annual land-cover maps
Google Earth Engine
Land abandonment
Land-use change
Signature extension
Training data generation

ABSTRACT

Cropland abandonment is a widespread land-use change, but it is difficult to monitor with remote sensing because it is often spatially dispersed, easily confused with spectrally similar land-use classes such as grasslands and fallow fields, and because post-agricultural succession can take different forms in different biomes. Due to these difficulties, prior assessments of cropland abandonment have largely been limited in resolution, extent, or both. However, cropland abandonment has wide-reaching consequences for the environment, food production, and rural livelihoods, which is why new approaches to monitor long-term cropland abandonment in different biomes accurately are needed. Our goals were to 1) develop a new approach to map the extent and the timing of abandoned cropland using the entire Landsat time series, and 2) test this approach in 14 study regions across the globe that capture a wide range of environmental conditions as well as the three major causes of abandonment, i.e., social, economic, and environmental factors. Our approach was based on annual maps of active cropland and non-cropland areas using Landsat summary metrics for each year from 1987 to 2017. We streamlined per-pixel classifications by generating multi-year training data that can be used for annual classification. Based on the annual classifications, we analyzed land-use trajectories of each pixel in order to distinguish abandoned cropland, stable cropland, non-cropland, and fallow fields. In most study regions, our new approach separated abandoned cropland accurately from stable cropland and other classes. The classification accuracy for abandonment was highest in regions with industrialized agriculture (area-adjusted F1 score for Mato Grosso in Brazil: 0.8; Volgograd in Russia: 0.6), and drylands (e.g., Shaanxi in China, Nebraska in the U.S.: 0.5) where fields were large or spectrally distinct from non-cropland. Abandonment of subsistence agriculture with small field sizes (e.g., Nepal: 0.1) or highly variable climate (e.g., Sardinia in Italy: 0.2) was not accurately mapped. Cropland abandonment occurred in all study regions but was especially prominent in developing countries and formerly socialist states. In summary, we present here an approach for monitoring cropland abandonment with Landsat imagery, which can be applied across diverse biomes and may thereby improve the understanding of the drivers and consequences of this important land-use change process.

1. Introduction

Cropland abandonment is a common type of land-use change across the globe and can be caused by a range of social, economic, and environmental factors (Hatna and Bakker, 2011; Li and Li, 2017; MacDonald et al., 2000). For example, during the 20th century broad-scale cropland abandonment has occurred in Europe (Hatna and Bakker, 2011; Pinto Correia, 1993; Walther, 1986), North America (Brown et al., 2005; Flinn et al., 2005; Ramankutty and Foley, 1999), and East Asia (Osawa et al., 2016; Shoyama and Braimoh, 2011; Su et al., 2018). In recent decades, developing regions such as China (Ladikas et al., 2009; Wang et al., 2015), Latin America (Díaz et al., 2011; Grau and Aide, 2008; Laue and Arima, 2016), and Southeast Asia (Li et al., 2017; Yusoff et al., 2015) have experienced high rates of cropland abandonment. In general, marginal croplands, for example in mountains, afar from transportation routes or markets, and on poor

* Corresponding author.
E-mail address: hyin3@kent.edu (H. Yin).

https://doi.org/10.1016/j.rse.2020.111873
Received 5 November 2019; Received in revised form 14 April 2020; Accepted 6 May 2020
Available online 23 May 2020

soils are especially prone to abandonment because they tend to be less profitable (Gellrich and Zimmermann, 2007; Mottet et al., 2006). Factors, such as land reforms (Kuemmerle et al., 2008), land degradation (O'Hara, 1997), and armed conflicts (Yin et al., 2019) can trigger cropland abandonment even in areas that are well suited for agriculture.

Cropland abandonment has wide-ranging effects on the environment, especially on biodiversity and carbon storage (Cramer et al., 2008; Isbell et al., 2019; Munroe et al., 2013). For biodiversity conservation, cropland abandonment can either be a threat or an opportunity (Queiroz et al., 2014). Wildlife communities adapted to agroecosystems may decline, but those favoring early-successional vegetation typically flourish. Similarly, carbon stocks depleted by exploitative agricultural practices may recover as succession progresses and soils are replenished with organic matter (Vuichard et al., 2008). However, environmental outcomes depend on the time since abandonment. For example, species richness and composition vary by successional stage (Baba et al., 2019; Isbell et al., 2019). Similarly, carbon sequestration rates are generally faster soon after abandonment than in later years (Poeplau et al., 2011; Wertebach et al., 2017). Therefore it is necessary to identify both the extent and the timing of abandonment when predicting its environmental consequences (Kolecka, 2018).

Despite the importance of cropland monitoring, cropland abandonment is difficult to map and not routinely monitored. One option to assess cropland abandonment is to rely on statistics released by national or international organizations such as the Food and Agriculture Organization of the United Nations (FAO) that report the annual extent of active croplands at regional, national, and subnational levels (e.g., FAOSTAT). However, such aggregated statistics cannot capture the spatial pattern of changes nor the detailed change process such as abandonment and expansion.

Mapping cropland change from satellite imagery is better suited to capture the spatial patterns of changes, but it is difficult because of the complexity of cropland abandonment. Taking advantage of all available satellite imagery, several time series algorithms, such as Landsat-based detection of trends in disturbance and recovery (LandTrendr, Kennedy et al., 2010), Breaks For Additive Season and Trend (BFAST, Verbesselt et al., 2010), and Continuous Change Detection and Classification (CCDC, Zhu and Woodcock, 2014) have been developed and applied to monitor land surface change at frequent time intervals. These trajectory-based methods are typically applied to indices derived from a certain number of spectral bands, such as Normalized Difference Vegetation Index (NDVI), Normalized Burn Ratio (NBR) or Tasseled Cap (TC) components to monitor changes within a certain land cover class (e.g. forest change). However, one challenge for these algorithms is to capture land cover conversions accurately when the land cover class at either time point varies greatly in spectral reflectance. In the case of cropland abandonment, the changes in spectral reflectance stemming from abandonment can differ greatly depending on the crop types prior to abandonment and the successional pathways thereafter. Moreover, mapping abandonment is confounded by different definitions of "abandonment". Abandoned cropland is often defined as cropland that has not been cultivated for at least two to 5 years (FAO, 2016; Pointereau et al., 2008), but if the period without cultivation is short, then abandoned cropland is easily confused with crop rotations that include fallow periods. Furthermore, prior attempts to map abandonment have largely relied on pairs of multi-date satellite imagery (Liu et al., 2014; Prishchepov et al., 2012; Witmer, 2008) that do not fully capture the temporal dynamics that define abandonment (Estel et al., 2015). As a result, often only areas where succession had already progressed to the stage of woody vegetation were deemed abandoned. Ideally, abandonment maps should be based on long-term time series of satellite imagery with frequent observations.

Sensor limitations, especially coarse resolution, further complicate cropland abandonment mapping. Coarse resolution (> 250 m) satellite data acquired by AVHRR, SPOT-Vegetation or MODIS sensors are important for cropland mapping because of their high temporal resolution and global coverage (DeFries et al., 1998; Friedl et al., 2002). However, coarse-resolution imagery is problematic when mapping small agricultural fields (Fritz et al., 2015). Medium-resolution imagery, e.g., from Landsat and Sentinel-2, allows to monitor of croplands at a finer spatial scale (Defourny et al., 2019; Thenkabail et al., 2012). Prior maps of cropland abandonment based on medium-resolution data mostly focus on small extents and limited time periods (Grădinaru et al., 2016; Parés-Ramos et al., 2008) due to the challenge of processing medium-resolution data for large areas efficiently. Cloud based geo-processing platforms, such as Google Earth Engine (Gorelick et al., 2017), may alleviate some of these limitations and improve cropland abandonment mapping based on medium-resolution imagery.

The challenge of obtaining good training data for classifying satellite image also hampers cropland abandonment mapping. To separate cropland abandonment from crop rotations that include fallow periods, a consistent time series of cropland maps is necessary, but such maps are rarely available. This is largely due to the lack of ground reference data that can be used to train classifiers (Fritz et al., 2012; Gómez et al., 2016). Training data relates the response (i.e., land-cover class assignment) to the spectral reflectance in corresponding satellite images. However, the spectral reflectance of agricultural land use often differs from year to year, e.g., because of changes in crop types, making it challenging to build a generalized classifier (Laborte et al., 2010; Xu et al., 2018). Baring other approaches, it would be necessary to collect a unique set of training data for each year that is to be classified, but that is very labor intensive, and prohibitive for mapping large spatial extents.

Signature extension (also referred to as signature generalization) can overcome the need for annual training data when producing consistent time series of land cover. Signature extension applies a predictive model built from training data obtained from one domain (e.g., in space, time, or by sensor) to another (Chittineni, 1980; Olthof et al., 2005; Woodcock et al., 2001). Two groups of signature extension approaches exist and have been used to produce temporally consistent land-cover maps: 1) normalizing the imagery across time so that a classifier can be generalized to different years (Pax-Lenney et al., 2001); or 2) generating classifiers for individual years based on time-invariant classes (Fraser et al., 2009; Gray and Song, 2013). For cropland mapping, the first approach is not viable due to both strong phenological variation among years, and high within-class variance stemming from management, crop rotation, or intensification. The second approach, i.e., to parametrize a classifier for each year, does not require normalizing imagery to account for phenological difference, but requires stable land cover as training samples for annual classification (Dannenberg et al., 2016). It is this latter approach that shows the most promise for annual cropland mapping, and that we employed here.

Our goals were to develop an approach to map the extent and the timing of abandoned cropland using the entire Landsat time series and test this approach in 14 study regions across the globe that capture a wide range of environmental conditions as well as the three major causes of abandonment, i.e., social, economic, and environmental factors. To do so, we

a) developed an approach for generating a set of training samples for annual classifiers with minimal *a priori* information;
b) produced annual cropland maps based on summary metrics derived from Landsat time series;
c) mapped patterns and timing of cropland abandonment by differentiating abandonment from stable cropland, stable non-cropland, and short-term fallow land.

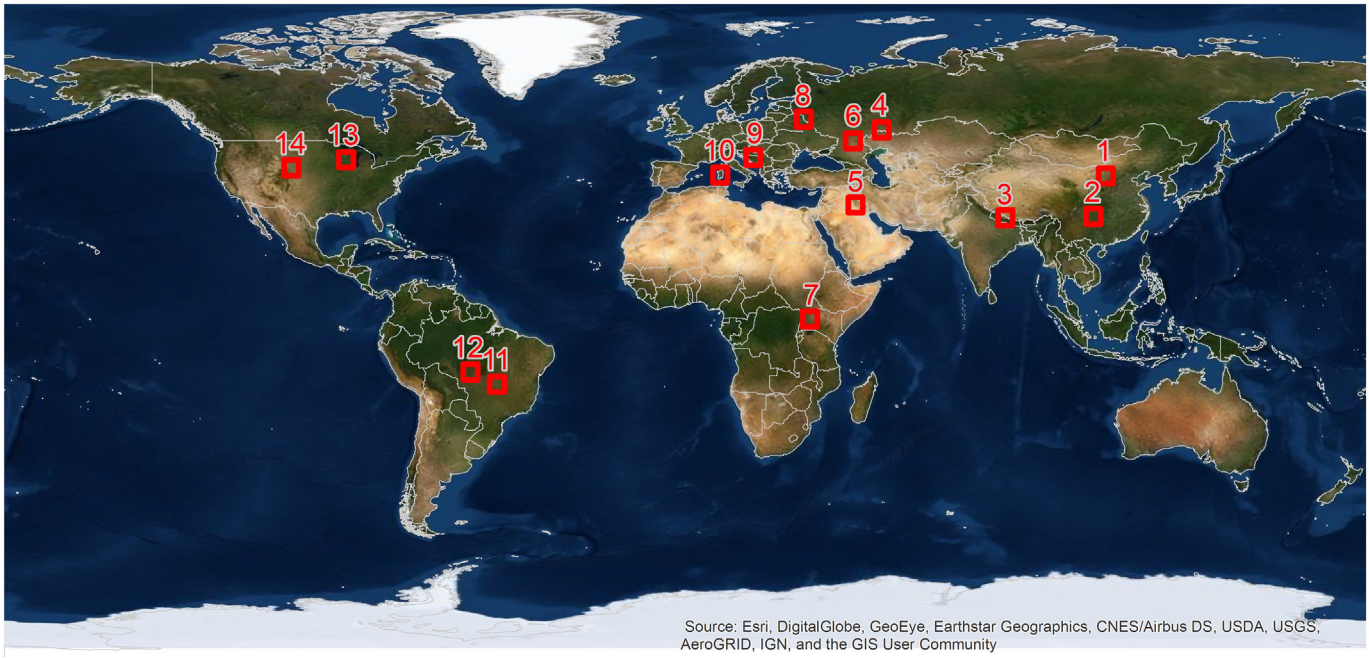

Fig. 1. Study regions: 1. Shaanxi (China), 2. Chongqing (China), 3. Nepal, 4. Orenburg (Russia), 5. Iraq, 6. Volgograd (Russia), 7. Uganda, 8. Belarus, 9. Bosnia and Herzegovina, 10. Sardinia (Italy), 11. Goias (Brazil), 12. Mato Grosso (Brazil), 13. Wisconsin (USA), 14. Nebraska (USA).

2. Methods

2.1. Study areas

We mapped cropland abandonment in 14 study regions (Fig. 1, Table 1), ranging from drylands (Iraq, Nebraska, Shannxi, Orenburg, Uganda), to temperate regions (Belarus, Bosnia and Herzegovina, Sardinia, Volgograd, Wisconsin), to the sub-tropic and wet tropics (Chongqing, Goias, Mato Grosso, Nepal). We selected these test regions also because of their documented histories of cropland abandonment in the past three decades (Suppl. A). Our study regions captured a diverse mix of three potential abandonment drivers including social (e.g., Shannxi, Bosnia and Herzegovina), economic (e.g., Chongqing, Sardinia), and environmental change (e.g., Iraq, Nepal). For detailed descriptions of each study region, please see the Supplementary files (Suppl. A).

2.2. Class definition

We based our method for mapping cropland abandonment on annual land-cover maps. We defined 'active cropland' as areas that are used to grow row crops and are typically tilled, resulting in a clear soil signal at some point during the year. Accordingly, our cropland definition did not include some croplands that are used to produce perennial crops and those that are not tilled. We expect this potential omission to be relatively small as most crops are annually harvested (Monfreda et al., 2008) and tilled (Porwollik et al., 2019). 'Herbaceous vegetation' was defined as any unplowed area that is not dominated by shrubs or trees. 'Woody vegetation' was defined as areas where shrubs and trees were dominant. 'Non-vegetated' included water, barren land, urban areas, and other areas devoid of vegetation.

The annual maps allowed us to identify cropland abandonment by assessing land-cover trajectories through time. We defined cropland as abandoned if the land was not cultivated for at least five consecutive years, which is a conservative definition employed by the United Nations' Food and Agriculture Organization (FAO, 2016). We defined fallow as croplands not cultivated for < 5 consecutive years after a period of consistent cultivation (FAO, 2016). Our approach can be easily adapted to accommodate alternative definitions of abandonment that use shorter thresholds.

Table 1
The study regions that we selected, the biome that they are part of, and the major causes for abandonment in each region.

No.	Location	Biome	Major causes of abandonment
1	Shaanxi (China)	Semi-arid	Grain for Green program; Rural out-migration
2	Chongqing (China)	Subtropics	Urbanization; Rural out-migration
3	Nepal	Alpine-subtropics	Climate change; Rural out-migration; Off-farm employment
4	Orenburg (Russia)	Semi-arid	Collapse of socialism (economic crises)
5	Iraq	Arid	Armed conflicts; Soil salinization
6	Volgograd (Russia)	Semi-arid	Collapse of socialism (economic crises)
7	Uganda	Tropical Savana	Armed conflicts
8	Belarus	Temperate	Collapse of socialism (institutional change)
9	Bosnia and Herzegovina	Temperate	Collapse of socialism; Armed conflicts
10	Sardinia (Italy)	Mediterranean	Economy transition; Rural-outmigration
11	Goias (Brazil)	Tropics	Farm consolidation; Commodity price; Land mismanagement
12	Mato Grosso (Brazil)	Tropics	Forest conservation policies
13	Wisconsin (USA)	Temperate	Farm consolidation
14	Nebraska (USA)	Semi-arid	Conservation Reserve Program; Commodity price

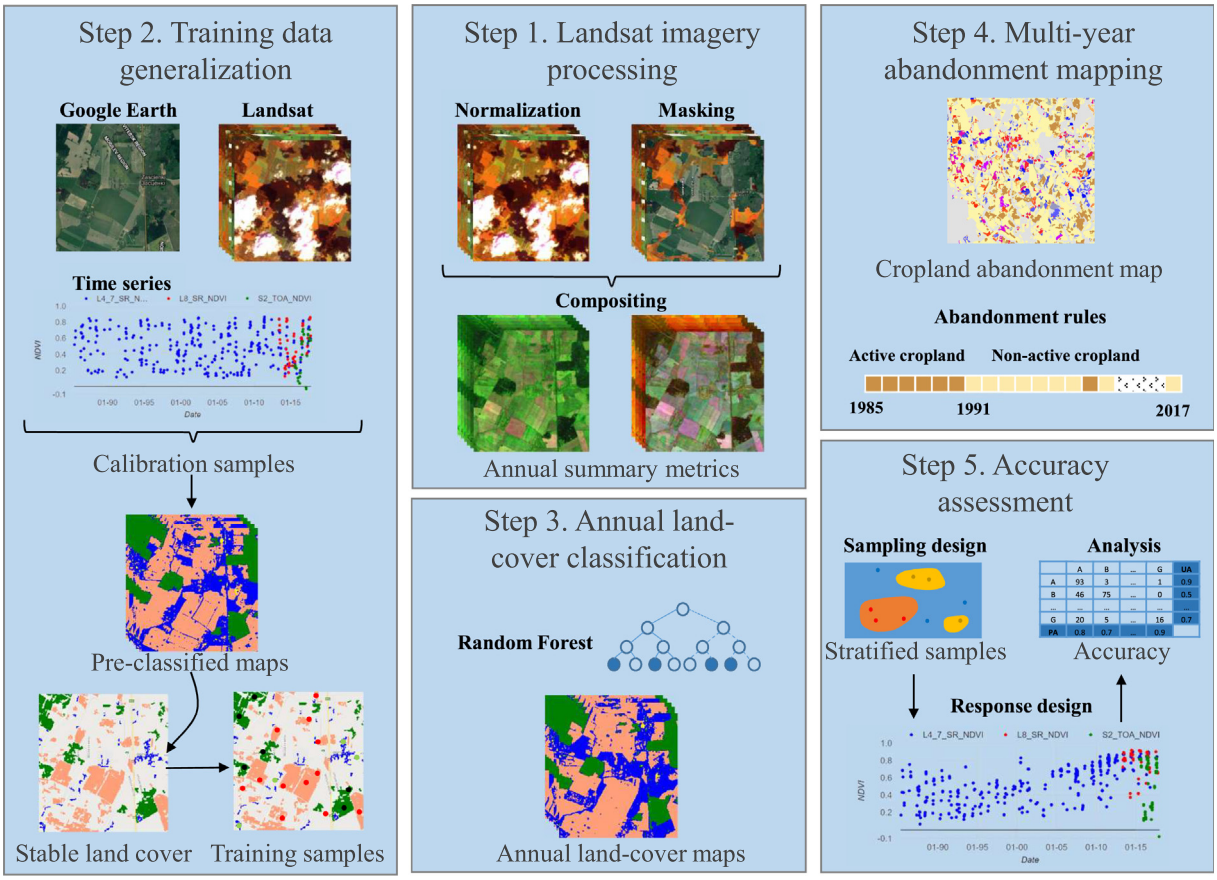

Fig. 2. Flowchart of the data analysis.

2.3. Data analysis

Our abandonment mapping approach consisted of five steps (Fig. 2). In the first step, we created annual summary metrics from the Landsat imagery (Section 2.3.1). Second, we collected a small set of calibration samples by visually interpreting Landsat and Sentinel-2 time series and high-resolution satellite imagery in Google Earth. The calibration samples were stable in terms of their land cover, i.e., always cropland or always woody vegetation from 1986 to 2018 (Section 2.3.2). Using the calibration samples, we pre-classified annual summary metrics using a random forest classifier and identified pixels with stable land cover across the annual classifications. As part of this step, we conducted a sensitivity analysis to test how many calibration samples were necessary for accurate classifications. We then generated training data from these stable areas. Third, we used these training data to train final random forest classifiers for each region and each year to produce annual land-cover maps (Section 2.3.3). We validated the annual land-cover maps for all study regions by assessing accuracy of regional maps produced for the year 2015. For Nebraska and Wisconsin, we also used the Cropland Data Layer (CDL) (Boryan et al., 2011) for validation. Moreover, using Shaanxi study region as an example, we tested how Landsat data density influenced mapping accuracy. Fourth, we distinguished cropland abandonment from stable cropland, fallow, and non-cropland based on the temporal trajectory of the land cover of each pixel (Section 2.3.4). Finally, in step five, we estimated the mapping accuracy of the cropland abandonment map based on an error-adjusted stratified estimator (Section 2.3.5). We performed all data analyses in Google's Earth Engine (Gorelick et al., 2017).

2.3.1. Landsat imagery processing

We analyzed all available Landsat Tier 1 surface reflectance imagery from 1986 to 2018 that was available for each of our study regions in Google Earth Engine as of April 2019. These data were atmospherically corrected by the USGS using LEDAPS (Masek et al., 2006) and LaSRC (Vermote et al., 2016), and masked to exclude clouds, cloud shadows, and snow/ice using the accompanying quality assessment band. Due to differences in the spectral reflectance of OLI relative to the previous sensors, we applied the coefficients from Roy et al. (2016) to normalize OLI reflectance to that of TM and ETM+. With the exception of Uganda, all study regions had at least one cloud-free image in each year since 1985. Because of the limited data availability for our Uganda study region, we were only able to examine imagery 1998 to 2017 there.

We calculated annual summary metrics from the full Landsat data record as input variables for our classifications. Summary statistics that describe the distribution of the data over time can improve land cover mapping (Potapov et al., 2012; Yin et al., 2017). Moreover, calculating metrics based on imagery from multiple years improves the mapping of dynamic classes such as cropland (Pflugmacher et al., 2019), which is why we included imagery from ± 1 year to calculate metrics for each target year. For instance, we included all available images from 1986 to 1988 when generating metrics for the target year 1987. The observation density in the study regions suggested that by using a three-year window we were able to calculate summary metrics at annual intervals even for periods that had relatively few observations (e.g., 1990s) (Suppl. B, Fig. S1).

We calculated the following summary metrics: maximum, minimum, mean, median, standard deviation, and the 20th and 80th percent quantile for each spectral band and for six indices. The indices were: Bare Soil Index (BSI), Normalized Burn Ratio (NBR), Normalized Difference Vegetation Index (NDVI), Brightness, Greenness, and Wetness from a Tasseled Cap Transformation. BSI was originally

Table 2
Coefficients for the Tasseled Cap Transformation for the Landsat TM, ETM+ and the normalized OLI (Crist, 1985).

Feature	Blue	Green	Red	NIR	SWIR1	SWIR2
Brightness	0.2043	0.4158	0.5524	0.5741	0.3124	0.2303
Greenness	−0.1603	−0.2819	−0.4934	0.7940	−0.0002	−0.1446
Wetness	0.0315	0.2021	0.3102	0.1594	−0.6806	−0.6109

developed for forestry applications to differentiate bare soil from other land-cover classes (Rikimaru et al., 2002). We included BSI to capture the soil signal when croplands were tilled or harvested (Diek et al., 2017). BSI values range from −1 to 1, where a higher value indicates higher soil bareness.

$$BSI = \frac{(\text{SWIR2} + \text{red}) - (\text{NIR} - \text{blue})}{(\text{SWIR2} + \text{red}) + (\text{NIR} - \text{blue})}$$

We calculated NDVI based on the normalized difference between the red and near infrared bands. NBR was calculated based on the normalized difference between the near infrared and short-wave bands (SWIR2). We used the coefficients provided by Crist (1985) for the Tasseled Cap Transformation (Table 2). While Crist's coefficients were original designed for Landsat TM, to the best of our knowledge, there are no existing coefficients available for calculating Tasseled Cap coefficients from OLI surface reflectance, only for OLI top of atmosphere radiance (Baig et al., 2014). Thus, we normalized OLI reflectance so that it matched TM and ETM+ data using the coefficients from Roy et al. (2016) before we applied Crist's coefficients.

2.3.2. Training data generation

In order to generate training samples, we developed an approach for identifying pixels that were stable in terms of their land cover over the entire Landsat image record. We applied our approach separately in each study region, and ultimately parameterized a unique classifier for each year in each study region.

Our first step was to collect a small set of calibration samples based on the visual interpretation of imagery time series. These calibration samples were Landsat pixels that had the same land-cover class in all years. To identify and label these samples, we developed a Time Series Viewer tool on Google Earth Engine (available at https://github.com/hyinhe/GEE-codes). Our samples were selected based on visual examination of time series of the BSI, NBR, NDVI, Brightness, Greenness, Wetness, cloud-free Landsat 4–8 and Sentinel 2 imagery composites (RGB: NIR, SWIR1, red), plus high-resolution imagery available in Google Earth. We manually selected pixels in which visual interpretation suggested that the land cover was consistent throughout our study period. We excluded pixels where land cover changed, but retained cropland samples crop types changed (e.g., rotations) or productivity varied (see Suppl. B, Fig. S2). To identify the necessary sample size, we tested different sizes of calibration samples from 10 to 50 per land cover class in our test site in Shaanxi. The result showed that using > 40 samples increased mapping accuracy by < 1% (Suppl. B, Fig. S3). Thus, we decided to collect 50 calibration samples for each of the four land-cover classes.

Our second step was to use these calibration samples to classify annual sets of summary metrics for every third year (i.e., 1987, 1990, 1993, etc.) using a random forest classifier. From these classified land-cover maps, we identified areas that retained the same land-cover class across all years. We grouped neighboring pixels in the same land-cover class into polygons and omitted small polygon (< 1 ha, ≈ 11 Landsat pixels) to avoid spatial uncertainties due to mixed pixels and errors in image co-registration. From these stable areas we randomly selected 2000 Landsat pixels per class as training samples for the final annual classification for each region in each year.

2.3.3. Annual land-cover classification

We produced annual land-cover maps for each study region using a random forest classifier (Breiman, 2001). We trained the classifier separately for each test region and each year using the generated training samples. We set the number of variables that were randomly sampled as candidates at each split (*mtry*) to 9, which is the square root of the number of input variables, and the minimum size of the terminal nodes to 10.

2.3.4. Multi-year abandonment mapping

Based on our time series of annual land-cover maps with four land-cover classes (active cropland, herbaceous vegetation, woody vegetation, and non-vegetated), we identified stable cropland, fallow cropland, cropland abandonment, and others. First, we generated a map of stable cropland prior to 1990 (i.e., pixels classified as cropland in all years between 1987 and 1990). Within this cropland mask, we identified croplands as abandonment if a pixel was classified as non-cropland for at least five consecutive years. When abandonment occurred, we labeled its timing as the first year in which cropland was no longer active (starting from 1991 to 2013).

We mapped the cropland that was not actively managed consecutively for < 5 years as fallow, following the definition of FAO (2016). Also, we were conservative and included only those croplands as abandoned that converted to natural cover, not those that converted to urban or to water (e.g., due to new reservoirs). To do so, we masked out cropland conversions to urban based on the Joint Research Centre's Global Human Settlement Dataset (Pesaresi et al., 2015), and conversion to water based on the Global Surface Water Map (Pekel et al., 2016), both of which are available on Google Earth Engine.

2.3.5. Accuracy assessment

We quantified the accuracies of both our annual land-cover maps, and our abandonment maps. In order to assess the accuracy of our annual land-cover maps, we evaluated the maps for 2015 for each study region. We selected this year because of the widespread availability of high-resolution imagery on Google Earth for all of our study regions. We randomly selected a sample of 100 pixels for both cropland and non-cropland areas (i.e., herbaceous vegetation, woody vegetation, and non-veetated were considered collectively). Our sample size decision here was based on the recommendation from Congalton and Green (2009). We recorded the land-cover class of each sample by visually interpreting a) time series of Landsat-derived indices, b) multi-seasonal imagery from both Landsat, and c) high-resolution images available on Google Earth, which were acquired between 2014 and 2016. Our validation samples were labeled separately by 12 experts who had experiences with remote sensing data analysis. We instituted multiple training sessions with these 12 experts to ensure that the same criteria of sample labeling were followed. When a decision was difficult, a second opinion was obtained, and the sample was labeled collaboratively. Based on these assessed samples, we created confusion matrices for each study region and calculated producer's (PA), user's (UA), and overall accuracies (OA). We also calculated the F1 score ($F1 = 2 \times UA \times PA/(UA + PA)$) for the cropland class. The F1 score, a harmonic mean of user's and producer's accuracy, is advantageous when learning from imbalanced data (He and Ma, 2013; Powers, 2011). F1 score ranges from 0 to 1 with higher score indicating better classification performance.

We conducted additional tests to ensure the robustness of our annual classification approach. In order to understand the effect that the number of input Landsat images had on mapping accuracy, we randomly drew 10, 20, 30, 40, 50, 60, 70, 80 and 90% of all available imagery in 2015 for Shaanxi and calculated summary metrics for each set of imagery. We selected Shaanxi because its dense Landsat observations allowed us to test a wide range of imagery subsets (Suppl. B, Fig. S1). We then performed classification for each set of summary metrics using the same training data. We validated each land cover map

using the same validation samples and compared their mapping accuracies. The results of this exercise suggested that even when using only 10% of the imagery, we were able to achieve reliable classifications (Suppl. B, Fig. S4).

For our test regions in Nebraska and Wisconsin, we compared our cropland map with the U.S. Department of Agriculture's Cropland Data Layer (CDL) (Boryan et al., 2011). We used the binary cultivation layer from the CDL to validate our maps because of its high accuracy (PA: 93.9–98.8%, UA: 97.6–99.1%) (USDA NASS, 2018). The cultivation layers were available from 2013 to present, so we limited comparisons to our maps from 2013 to 2017. For each CDL cultivation layer, we randomly selected 100,000 pixels and used them to validate our cropland maps produced for Nebraska and Wisconsin. We reported the PA, UA and F1 score for each state and each year based on the error matrix built from 100,000 validation samples.

In order to validate our cropland abandonment maps, we applied disproportionate stratified sampling to assess small classes, such as cropland abandonment (Olofsson et al., 2014). In order to reduce the amount of validation samples needed, we aggregated abandonment classes into 3-year intervals so that a pixel in which abandonment occurred in either 1991, 1992, or 1993 was assigned to the aggregated abandonment class "1991–1993". To assess the accuracy of our abandonment maps, we randomly selected 150 pixels within each stable cropland, fallow, and non-cropland, as well as 50 pixels within each of the aggregated abandonment classes. While there are alternative recommendations in regards to appropriate size of validation samples (e.g. Olofsson et al., 2014), we used a stratified sampling strategy to reduce the efforts of sample collection that would be needed for the large number of change classes (Congalton and Green, 2009). Moreover, 50 validation samples for each abandonment class avoids the risk of small sample sizes for rare classes such as cropland abandonment that is inherent in simple random sampling. We visually interpreted these reference samples with the help of Landsat, Google Earth imagery, and time series of indices (i.e., NDVI, BSI, Tasseled-Cap Brightness, Greenness, and Wetness) in our Time Series Viewer, but without knowledge of the mapped class label. We created confusion matrices and calculated producer's and user's accuracies for both occurrence and timing of abandonment, as well as the F1 score for both the cropland abandonment class and overall accuracy, while accounting for possible sampling bias (Card, 1982).

3. Results

3.1. Annual cropland mapping

Our annual land-cover maps had overall accuracies ranging from 0.63 to 0.91 (Fig. 3) with the lowest in Uganda (overall accuracy: 0.63 ± 0.06, error bar represents a 95% confidence level) where land use was highly heterogeneous and many fields were smaller than the 30-m Landsat pixels. F1 scores for the other regions ranged from 0.52 to 0.94 (Fig. 4). The highest cropland mapping accuracies were found in Iraq (F1 score of cropland: 0.94), Mato Grosso (0.91), Belarus (0.91), Orenburg (0.91), and Nebraska (0.91), while cropland was less accurately mapped in Goias (0.65), Sardinia (0.65), Uganda (0.60), and Nepal (0.52). When comparing our cropland maps and the CDL cultivation layer, we found that our maps agreed well with the CDL data in Nebraska (average F1 score from 2013 to 2017 for cropland: 0.83) and Wisconsin (0.79) (Suppl. B, Fig. S5).

Visually, the annual land-cover maps, which were based on pixel-level classifications, had clear patterns of fields that corresponded to local terrain, climate, and socio-economic conditions (Fig. 4). For example, small cropland fields (< 1 ha) dominated the mountainous areas (e.g., Chongqing, Nepal) and areas where subsistence agriculture was common (e.g. Uganda). Conversely, large fields (> 100 ha) were dominant in areas with little topography and industrialized agriculture (e.g., Mato Grosso, Orenburg, and Nebraska).

3.2. Cropland abandonment mapping accuracy

Our approach for mapping cropland abandonment accurately separated cropland abandonment from other classes (Fig. 5). Most of the study regions had an overall accuracy ≥0.75, the exception being Uganda (0.23 ± 0.04).

For most study regions, the cropland abandonment maps were also accurate in assigning the year in which abandonment occurred, but accuracies varied depending on the environment, the type of agriculture, and the year (Fig. 6). In general, accuracies were the highest in regions with industrialized agriculture (average F1 score of abandonment year: Mato Groso: 0.8, Volgograd, and Belarus: 0.6) and drylands (e.g., Nebraska, and Shaanxi: 0.5). In contrast, accuracies were lowest where field sizes were small, for example, in mountains (e.g., Nepal: 0.1), and where agricultural land use varied greatly among years (e.g., Sardinia: 0.2).

3.3. Spatial and temporal pattern of cropland abandonment

The highly variable spatial patterns of abandonment that we observed among our study regions highlight the diverse nature of the abandonment process (Fig. 7; Suppl. B, Fig. S6-S8). Similarly, the temporal patterns of abandonment were different among study regions (Fig. 8; Suppl. B, Fig. S6-S8). In developing regions such as Shaanxi, Chongqing, and Nepal, abandonment rates generally increased through

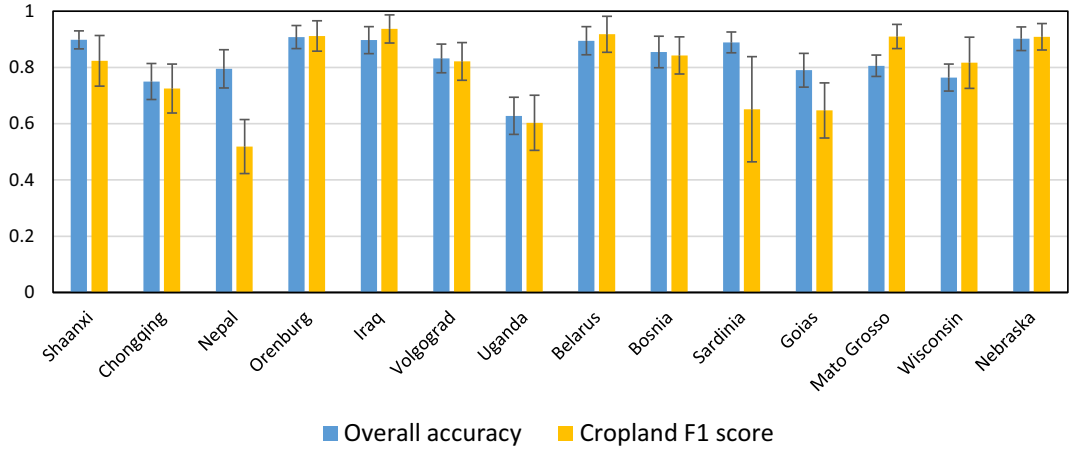

Fig. 3. Overall mapping accuracy and the F1 score for the cropland class in 2015. Error bars indicate 95% confidence intervals.

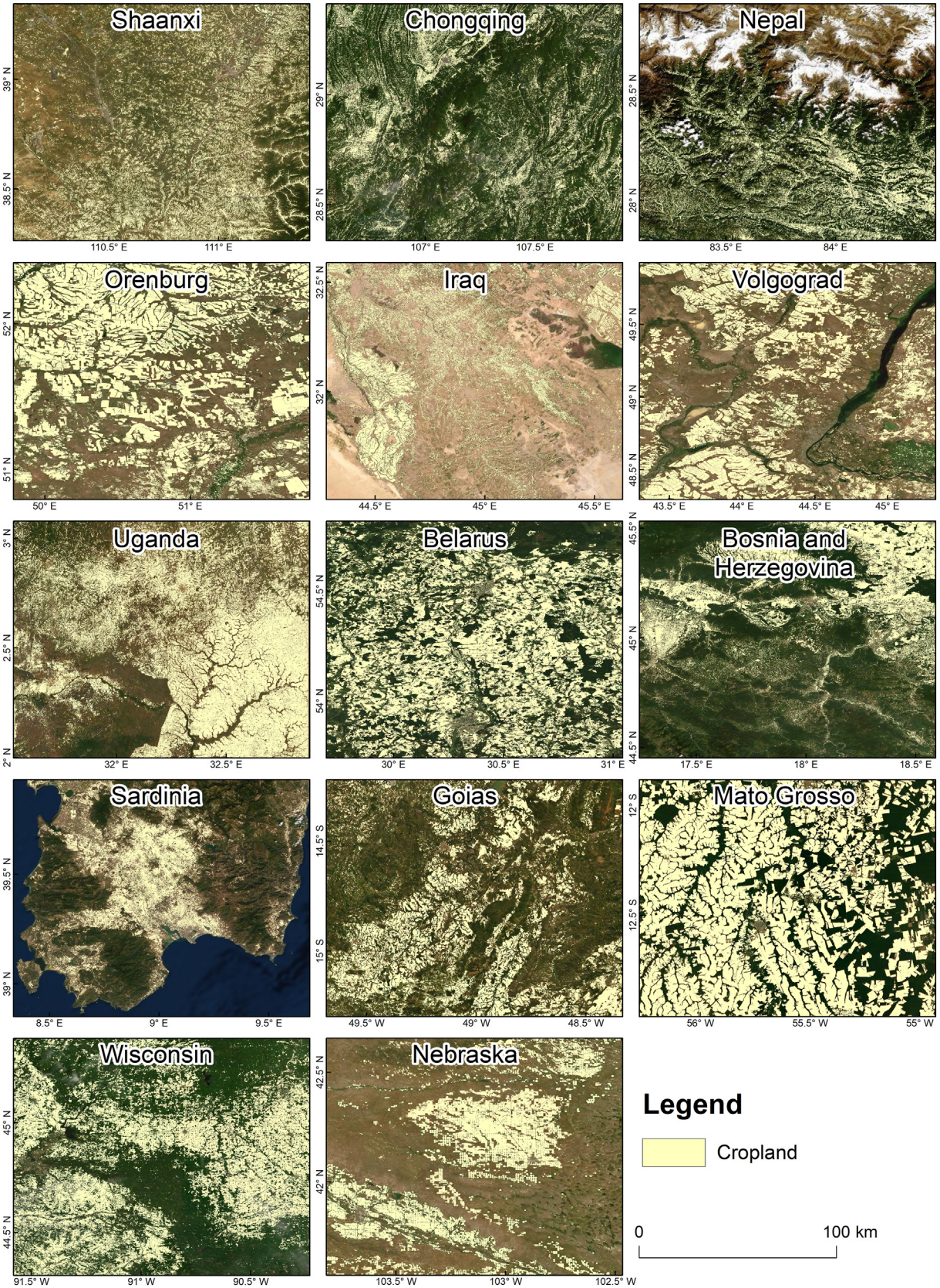

Fig. 4. Subsets of the 2015 land-cover maps showing the cropland in each study region with high-resolution imagery from Bing aerial in the background.

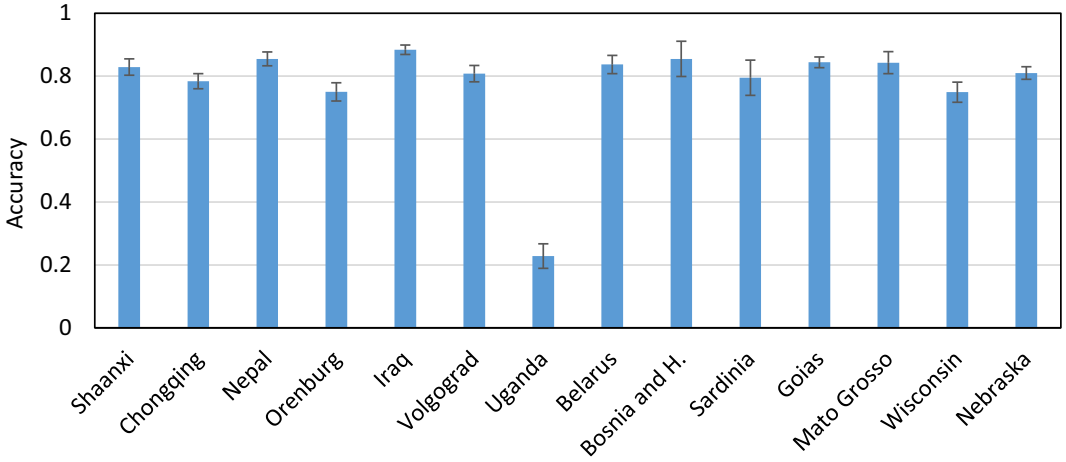

Fig. 5. Overall accuracy of the cropland abandonment map of each study region. Error bars indicate the 95% confidence intervals.

time but with large temporal fluctuations. Cropland abandonment rates in Shaanxi, for example, spiked between 2000 and 2005, declined between 2006 and 2008, and increased again after 2009. In contrast, in former socialist states in Eastern Europe, such as Belarus, Bosnia and Herzegovina, and Russia (Orenburg and Volgograd), abandonment rates were highest during the 1990s and declined gradually thereafter. In Brazil (Goias, Mato Grosso) and the US (Wisconsin, Nebraska), cropland abandonment rates were generally much lower. The highest temporal variations in abandonment occurred in Iraq, Uganda, and Sardinia where climate variability is high and affects the persistence of agriculture.

4. Discussion

We present here a new method to map cropland abandonment patterns, including the year when abandonment occurred based on the full Landsat record, as well as the implementation of this method in 14 study regions across the globe. Our detection of cropland abandonment was based on annual land-cover classifications that we generated from all available Landsat imagery. To classify cropland annually, we developed an approach that generates training data for each year based on a small set of stable ground reference samples. Our approach does not assume that reflectance and phenology remains similar among years. The problem with the assumption of inter-annual similarity is that croplands may differ among years because of variations in phenology, crop type, climate, water availability, land-use intensity, and the dates for which satellite data are available. Our method overcomes these obstacles by generating a new random forest classifier for each year based on time-stable reference samples and therefore does not require spectral reflectance to be comparable among years. That makes our approach highly adaptive and it avoids erroneous change detection. As a result, we were able to generate consistent, annual maps of highly dynamic land-use classes such as cropland, without having to select training data for each year.

Our method allowed us to produce annual cropland maps for most of our study regions (cropland F1 score: 0.52–0.94). Mato Grosso, Belarus, Orenburg, and Nebraska had the highest mapping accuracy. However, in the study regions with small field sizes and low-intensive farms (e.g., Chongqing, Nepal, and Uganda), mapping accuracies were lower. For instance, Uganda has an average farm size of < 1 ha, and most fields are considerably smaller than that (Ker, 1995). Moreover, trees are common in agricultural fields because tilling is done by hand, and trees are planted or left for fruit, shade, firewood, and as windbreaks (Miller et al., 2017). As a result, the majority of Landsat pixels in this region are mixtures of cropland, herbaceous land, and woody vegetation. Consequently, we were not able to map cropland accurately here and our mapping accuracy for Uganda (cropland F1 score: 0.6) was similarly low as that of other cropland maps for Africa (e.g., Feng et al., 2018; Xu et al., 2018). In mountainous areas such as Nepal or Chongqing, small fields on terraces were difficult to map, and

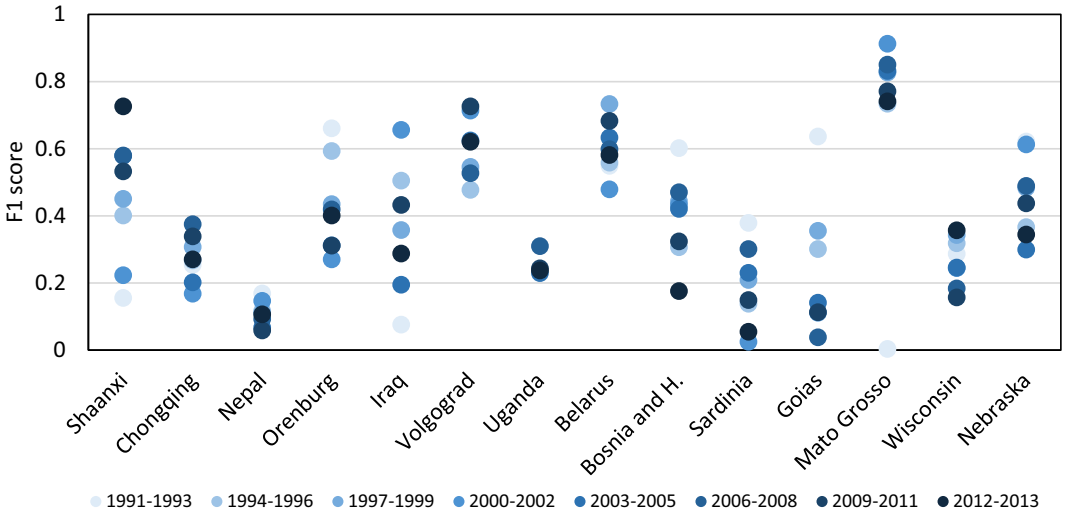

Fig. 6. The F1 score for the timing of cropland abandonment for all study regions.

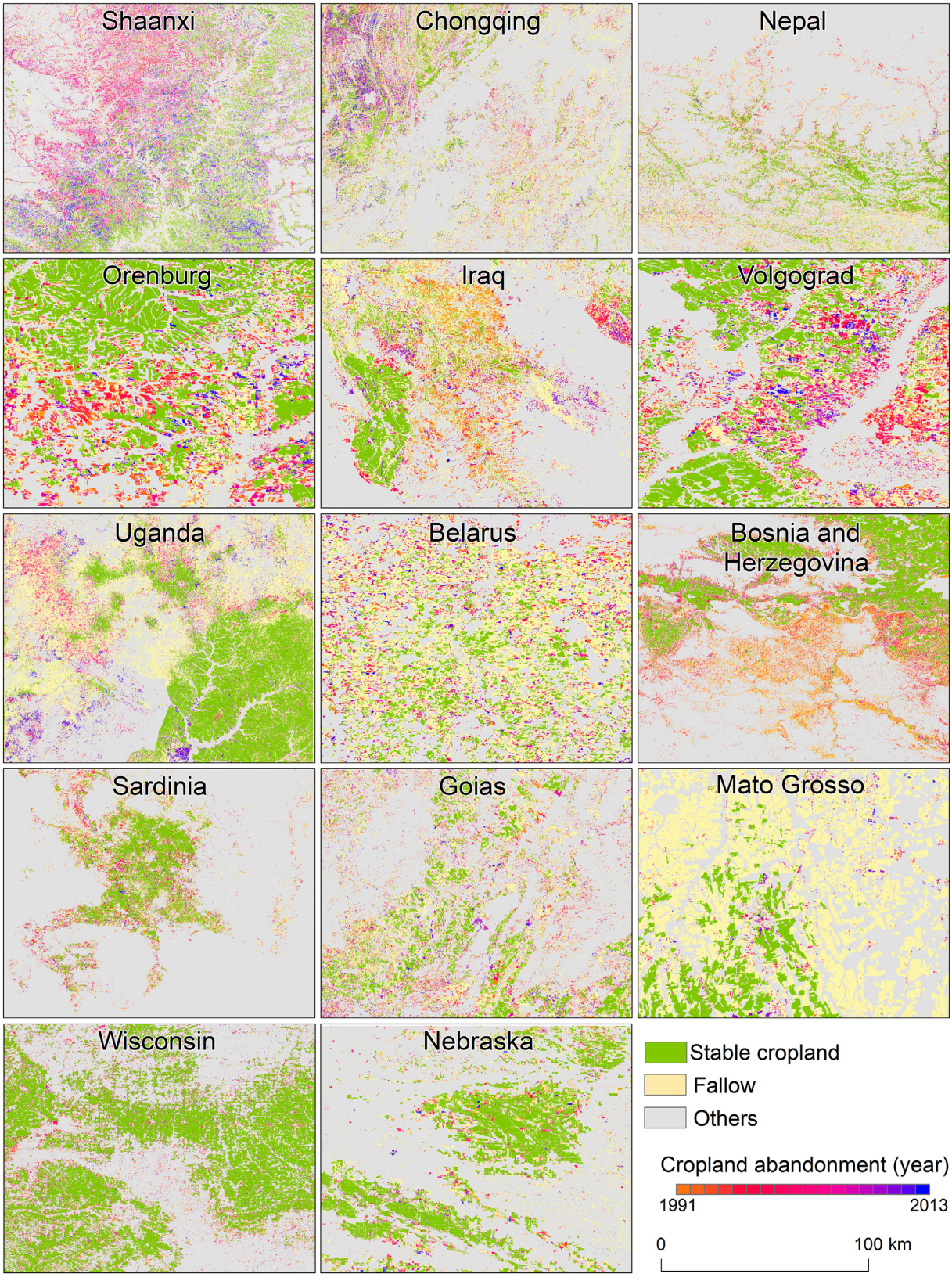

Fig. 7. The spatial pattern and the timing of cropland abandonment in the study regions.

topographic effects confounded our classifications (Vicente-Serrano et al., 2008). Mapping errors in cropland may also originate from the spectral similarly between cropland and herbaceous land such as grassland and wetland. While we did not explicitly investigate confusions between these two classes, previous studies suggested such possibility (Friedl et al., 2010; Wickham et al., 2013). Despite these limitations, our results generally demonstrated the potential of our approach for operational cropland mapping across large areas at annual

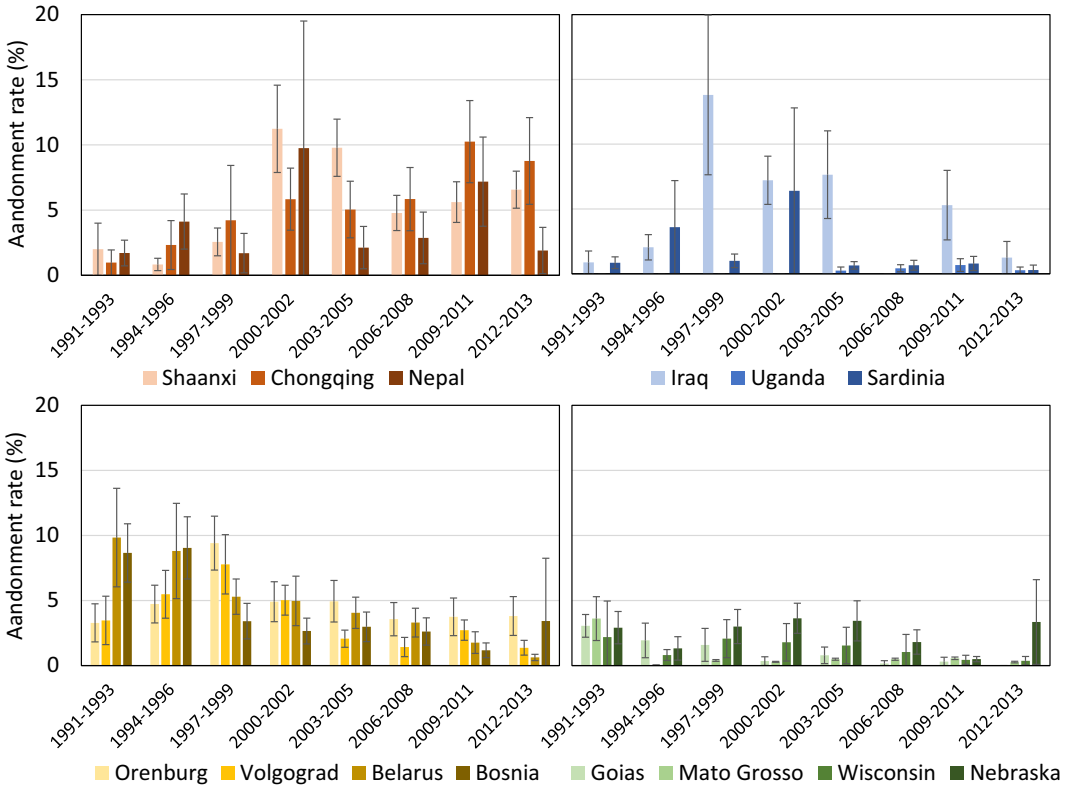

Fig. 8. The adjusted area estimates and associated 95% confidence intervals of cropland abandonment for the study regions from 1991 to 2013.

intervals.

We mapped cropland abandonment based on land-cover trajectories derived from our annual land-cover maps. The higher abandonment mapping accuracy in large and intensively managed croplands (e.g., Belarus and Volgograd) and drylands (e.g., Shaanxi, Nebraska) may be due to large spectral differences between active and non-active croplands, which facilitate better class separation. Conversely, mapping accuracy was lower in the study regions where cropland and non-cropland had similar spectral characteristics during the growing season. In Goias, for example, cropland and tilled-pasture are combined in agricultural rotations making it difficult to differentiate them (Carvalho et al., 2014; Mueller et al., 2015). Lastly, we observed some mapping errors due to the conversion from cropland to orchards, vineyards, and horticultural fields because our approach did not distinguish woody vegetation for production purposes from post-abandonment natural succession.

We found widespread cropland abandonment in most study regions, but the timing and area of abandoned croplands varying greatly. While we did not investigate the causes for abandonment directly, prior studies point to different causes of abandonment in the different regions. In Nepal, for example, urbanization and off-farm employment has caused rural outmigration and subsequent abandonment (Khanal and Watanabe, 2009). Similarly, in Chongqing, gradual cropland abandonment is due to decreases in rural populations and hence labor (Yan et al., 2016; Zhang et al., 2011). However, in Shaanxi land-use policy may have played a more important cause for abandonment (Lü et al., 2012; Zhou et al., 2012). For example in 2000, the Chinese government launched a series of programs aiming to restore vegetation cover by converting croplands in mountains and drylands to forests or grasslands. However, restoration efforts were reduced after 2004 due to concerns about China's food security (Yin et al., 2018a) and our maps show a subsequent decline in abandonment rates (Fig. 8). Similarly, the Conservation Reserve Program (CRP) in the U.S. rents cropland from farmers in 10–15 year contracts to cease cultivation of environmentally sensitive land (Hendricks and Er, 2018). CRP enrollment may thus explain some of the cropland abandonment we observed in Nebraska where CRP participation is high (Hiller et al., 2009). Finally, abrupt socio-economic changes can trigger cropland abandonment as did the breakdown of the Soviet Union in 1991 followed by the transition from a planned to a market-oriented economy (Prishchepov et al., 2013). Indeed, we observed high rates of abandonment in former socialist states in the 1990s.

Our approach may facilitate improved mapping of abandonment across diverse biomes and drivers. Prior to our study, we are aware of only two trajectory-based studies that mapped the timing of abandonment using Landsat data (Dara et al., 2018; Yin et al., 2018b), and our abandonment mapping accuracy was comparable to both. However, our approach does not require a specific threshold of change magnitude that separates abandonment from other classes. This has implication for mapping abandonment across a large range of biomes and agricultural systems where changes in spectral reflectance due to abandonment can differ greatly among regions (e.g., Suppl. B, Fig. S6-S8). Other prior efforts to map abandonment have limitations in that they either relied on coarse satellite data (Estel et al., 2015), analyzed only a few time points (Nguyen et al., 2018), or mapped early-successional woody vegetation and assumed that its presence reflected abandonment (Alcántara et al., 2013; Kolecka, 2018). The drawback of coarser spatial resolution is that it obscures many cropland changes when field sizes are less than pixel size (Ozdogan and Woodcock, 2006). Even with 30-m Landsat pixels, we encountered this issue, for example, in our Uganda study site. The drawback of mapping land abandonment based on only a few time points is that agricultural land use is much more dynamic, than, for example, forest use or urbanization, and abandonment phases are easily missed when analyzing decadal time steps. Finally, inferring abandonment from the presence of early successional woody vegetation is overly conservative because 5–10 years may pass before woody encroachment occurs (Potapov et al., 2015; Ruskule et al., 2012), and because it misses abandonment in drylands without a successional

trajectory towards woody vegetation (Löw et al., 2015). To overcome all of these shortcomings, our approach mapped land cover through time, making it suitable for both drylands and forested biomes.

Despite these strengths, our abandonment mapping approach has limitations that may limit its use for some applications. First, our abandonment mapping relies on high quality annual land cover maps that in turn required sufficient amount of imagery. We had at least eight observations per year in each of our 14 test regions (Suppl. B, Fig. S1), but that may not be the case elsewhere. Second, our approach relies upon a relatively small set of manually selected calibration samples, thus make our results vulnerable to the potential effects of mis-labeling. Errors in our calibration samples can propagate through classifications for all years and could reduce accuracy of mapped abandonment. Furthermore, it may be difficult to find stable samples if land cover change dominates in the region. Finally, we did not explicitly test our approach for mapping all types of cropland. While tilled croplands are widespread (Monfreda et al., 2008; Porwollik et al., 2019), there also exist perennial and no-till cropping systems, as well as systems that employ cover crops, and for all of these and there, the accuracy of our method for mapping abandonment may be lower. In regions where such systems are common, additional land cover classes, indices, or metrics should be considered. Ultimately, there may not be a one-size-fits-all method, but the flexibility of our approach makes it adaptable to a wide range of conditions.

5. Conclusion

Accurate maps of cropland abandonment are needed to understand the causes of agricultural land-use change and to mitigate the ecological and social-economic consequences of these changes. Unfortunately, there is a lack of approaches to reliably monitor cropland abandonment for large areas and across disparate biomes. Here, we present an approach for detecting where and when cropland abandonment has occurred based on annual classification of the entire Landsat record. We streamlined classifications with the generation of annual training samples. We tested our approach in 14 study regions representing a wide range of environmental conditions and land-use histories and different types of agriculture. Our results generally supported the reliability of our approach for detecting cropland abandonment, which resulted in accurate maps in most but not all study regions. Our approach does not assume that reflectance and phenology remain similar among years, thus is adaptive to each year and avoids erroneous change detection. However, small-scale farms and landscape heterogeneity pose challenges to abandonment mapping using medium resolution data such as Landsat. Ultimately, a global map of cropland abandonment is needed, and our work here demonstrates the potential for such a map and highlights the challenges to derive it.

Declaration of competing interest

The authors declare that they have no known competing financial interests or personal relationships that could have appeared to influence the work reported in this paper.

Acknowledgements

We gratefully acknowledge support for this research by the Land-Cover and Land-Use Change (LCLUC) Program of the National Aeronautics and Space Administration (NASA) through Grants NNX15AD93G and 80NSSC18K0316. We thank T. Allendorf, A. Prishchepov and K. Ostapowicz for discussions about agricultural abandonment, A. Kohansal for the suggestion of study region selection, and E. Bullock and P. Olofsson for the accuracy assessment tool on Google Earth Engine. We are grateful to four anonymous reviewers for their constructive comments.

Appendix A. Supplementary data

Supplementary data to this article can be found online at https://doi.org/10.1016/j.rse.2020.111873.

References

Alcántara, C., Kuemmerle, T., Baumann, M., Bragina, E.V., Griffiths, P., Hostert, P., Knorn, J., Müller, D., Prishchepov, A.V., Schierhorn, F., Sieber, A., Radeloff, V.C., 2013. Mapping the extent of abandoned farmland in central and Eastern Europe using MODIS time series satellite data. Environ. Res. Lett. 8, 035035. https://doi.org/10.1088/1748-9326/8/3/035035.

Baba, Y.G., Tanaka, K., Kusumoto, Y., 2019. Changes in spider diversity and community structure along abandonment and vegetation succession in rice paddy ecosystems. Ecol. Eng. 127, 235–244. https://doi.org/10.1016/J.ECOLENG.2018.12.007.

Baig, M.H.A., Zhang, L., Shuai, T., Tong, Q., 2014. Derivation of a tasselled cap transformation based on Landsat 8 at-satellite reflectance. Remote Sens. Lett. 5, 423–431. https://doi.org/10.1080/2150704X.2014.915434.

Boryan, C., Yang, Z., Mueller, R., Craig, M., 2011. Monitoring US agriculture: the US department of agriculture, national agricultural statistics service, cropland data layer program. Geocarto Int. 26, 341–358. https://doi.org/10.1080/10106049.2011.562309.

Breiman, L., 2001. Random forests. Mach. Learn. 45, 5–32.

Brown, D.G., Johnson, K.M., Loveland, T.R., Theobald, D.M., 2005. Rural land-use trends in the conterminous United States, 1950-2000. Ecol. Appl. https://doi.org/10.1890/03-5220.

Card, D.H., 1982. Using known map category marginal frequencies to improve estimates of thematic map accuracy. Photogramm. Eng. Remote. Sens. 48, 431–439.

Carvalho, J.L.N., Raucci, G.S., Frazão, L.A., Cerri, C.E.P., Bernoux, M., Cerri, C.C., 2014. Crop-pasture rotation: a strategy to reduce soil greenhouse gas emissions in the Brazilian Cerrado. Agric. Ecosyst. Environ. 183, 167–175. https://doi.org/10.1016/j.agee.2013.11.014.

Chittineni, C.B., 1980. Signature extension in remote sensing. Pattern Recogn. 12, 243–249. https://doi.org/10.1016/0031-3203(80)90064-3.

Congalton, R.G., Green, K., 2009. Assessing the Accuracy of Remotely Sensed Data: Principles and Practices, Second ed. CRC Press/Taylor & Francis, Boca Raton London New York. https://doi.org/10.1111/j.1477-9730.2010.00574_2.x.

Cramer, V.A., Hobbs, R.J., Standish, R.J., 2008. What's new about old fields? Land abandonment and ecosystem assembly. Trends Ecol. Evol. https://doi.org/10.1016/j.tree.2007.10.005.

Crist, E.P., 1985. A TM Tasseled cap equivalent transformation for reflectance factor data. Remote Sens. Environ. https://doi.org/10.1016/0034-4257(85)90102-6.

Dannenberg, M.P., Hakkenberg, C.R., Song, C., 2016. Consistent classification of landsat time series with an improved automatic adaptive signature generalization algorithm. Remote Sens. https://doi.org/10.3390/rs8080691.

Dara, A., Baumann, M., Kuemmerle, T., Pflugmacher, D., Rabe, A., Griffiths, P., Hölzel, N., Kamp, J., Freitag, M., Hostert, P., 2018. Mapping the timing of cropland abandonment and recultivation in northern Kazakhstan using annual Landsat time series. Remote Sens. Environ. https://doi.org/10.1016/j.rse.2018.05.005.

Defourny, P., Bontemps, S., Bellemans, N., Cara, C., Dedieu, G., Guzzonato, E., Hagolle, O., Inglada, J., Nicola, L., Rabaute, T., Savinaud, M., Udroiu, C., Valero, S., Bégué, A., Dejoux, J.-F., El Harti, A., Ezzahar, J., Kussul, N., Labbassi, K., Lebourgeois, V., Miao, Z., Newby, T., Nyamugama, A., Salh, N., Shelestov, A., Simonneaux, V., Traore, P.S., Traore, S.S., Koetz, B., 2019. Near real-time agriculture monitoring at national scale at parcel resolution: performance assessment of the Sen2-Agri automated system in various cropping systems around the world. Remote Sens. Environ. 221, 551–568. https://doi.org/10.1016/J.RSE.2018.11.007.

DeFries, R.S., Hansen, M., Townshend, J.R.G., Sohlberg, R., 1998. Global land cover classifications at 8 km spatial resolution: the use of training data derived from Landsat imagery in decision tree classifiers. Int. J. Remote Sens. 19, 3141–3168. https://doi.org/10.1080/014311698214235.

Díaz, G.I., Nahuelhual, L., Echeverría, C., Marín, S., 2011. Drivers of land abandonment in Southern Chile and implications for landscape planning. Landsc. Urban Plan. 99, 207–217. https://doi.org/10.1016/j.landurbplan.2010.11.005.

Diek, S., Fornallaz, F., Schaepman, M., de Jong, R., Diek, S., Fornallaz, F., Schaepman, M.E., de Jong, R., 2017. Barest pixel composite for agricultural areas using Landsat time series. Remote Sens. 9, 1245. https://doi.org/10.3390/rs9121245.

Estel, S., Kuemmerle, T., Alcántara, C., Levers, C., Prishchepov, A., Hostert, P., 2015. Mapping farmland abandonment and recultivation across Europe using MODIS NDVI time series. Remote Sens. Environ. 163, 312–325. https://doi.org/10.1016/J.RSE.2015.03.028.

FAO, 2016. FAOSTAT, Methods & Standards. [WWW Document]. URL. http://www.fao.org/ag/agn/nutrition/Indicatorsfiles/Agriculture.pdf.

Feng, D., Yu, L., Zhao, Y., Cheng, Y., Xu, Y., Li, C., Gong, P., 2018. A multiple dataset approach for 30-m resolution land cover mapping: a case study of continental Africa. Int. J. Remote Sens. 39, 3926–3938. https://doi.org/10.1080/01431161.2018.1452073.

Flinn, K.M., Vellend, M., Marks, P.L., 2005. Environmental causes and consequences of forest clearance and agricultural abandonment in Central New York, USA. J. Biogeogr. https://doi.org/10.1111/j.1365-2699.2004.01198.x.

Fraser, R.H., Olthof, I., Pouliot, D., 2009. Monitoring land cover change and ecological integrity in Canada's national parks. Remote Sens. Environ. 113, 1397–1409. https://doi.org/10.1016/j.rse.2008.06.019.

Friedl, M.A., McIver, D.K., Hodges, J.C.F., Zhang, X.Y., Muchoney, D., Strahler, A.H.,

Woodcock, C.E., Gopal, S., Schneider, A., Cooper, A., Baccini, A., Gao, F., Schaaf, C., 2002. Global land cover mapping from MODIS: algorithms and early results. Remote Sens. Environ. 83, 287–302.
Friedl, M.A., Sulla-Menashe, D., Tan, B., Schneider, A., Ramankutty, N., Sibley, A., Huang, X.M., 2010. MODIS collection 5 global land cover: algorithm refinements and characterization of new datasets. Remote Sens. Environ. 114, 168–182. https://doi.org/10.1016/j.rse.2009.08.016.
Fritz, S., McCallum, I., Schill, C., Perger, C., See, L., Schepaschenko, D., van der Velde, M., Kraxner, F., Obersteiner, M., 2012. Geo-Wiki: an online platform for improving global land cover. Environ. Model. Softw. 31, 110–123. https://doi.org/10.1016/j.envsoft.2011.11.015.
Fritz, S., See, L., McCallum, I., You, L., Bun, A., Moltchanova, E., Duerauer, M., Albrecht, F., Schill, C., Perger, C., Havlik, P., Mosnier, A., Thornton, P., Wood-Sichra, U., Herrero, M., Becker-Reshef, I., Justice, C., Hansen, M., Gong, P., Abdel Aziz, S., Cipriani, A., Cumani, R., Cecchi, G., Conchedda, G., Ferreira, S., Gomez, A., Haffani, M., Kayitakire, F., Malanding, J., Mueller, R., Newby, T., Nonguierma, A., Olusegun, A., Ortner, S., Rajak, D.R., Rocha, J., Schepaschenko, D., Schepaschenko, M., Terekhov, A., Tiangwa, A., Vancutsem, C., Vintrou, E., Wenbin, W., van der Velde, M., Dunwoody, A., Kraxner, F., Obersteiner, M., 2015. Mapping global cropland and field size. Glob. Chang. Biol. 21, 1980–1992. https://doi.org/10.1111/gcb.12838.
Gellrich, M., Zimmermann, N.E., 2007. Investigating the regional-scale pattern of agricultural land abandonment in the Swiss mountains: a spatial statistical modelling approach. Landsc. Urban Plan. https://doi.org/10.1016/j.landurbplan.2006.03.004.
Gómez, C., White, J.C., Wulder, M.A., 2016. Optical remotely sensed time series data for land cover classification: a review. ISPRS J. Photogramm. Remote Sens. 116, 55–72. https://doi.org/10.1016/J.ISPRSJPRS.2016.03.008.
Gorelick, N., Hancher, M., Dixon, M., Ilyushchenko, S., Thau, D., Moore, R., 2017. Google Earth Engine: planetary-scale geospatial analysis for everyone. Remote Sens. Environ. 202, 18–27. https://doi.org/10.1016/J.RSE.2017.06.031.
Grădinaru, S.R., Kienast, F., Psomas, A., 2016. Using multi-seasonal Landsat imagery for rapid identification of abandoned land in areas affected by urban sprawl. Ecol. Indic. https://doi.org/10.1016/j.ecolind.2017.06.022.
Grau, H.R., Aide, M., 2008. Globalization and land-use transitions in Latin America. Ecol. Soc. https://doi.org/10.5751/ES-02559-130216.
Gray, J., Song, C.H., 2013. Consistent classification of image time series with automatic adaptive signature generalization. Remote Sens. Environ. 134, 333–341. https://doi.org/10.1016/j.rse.2013.03.022.
Hatna, E., Bakker, M.M., 2011. Abandonment and expansion of arable land in Europe. Ecosystems. https://doi.org/10.1007/s10021-011-9441-y.
He, H., Ma, Y., 2013. Imbalanced learning: foundations, algorithms, and applications. In: Imbalanced Learning: Foundations, Algorithms, and Applications. John Wiley & Sons, Inc., Hoboken, N.J.. https://doi.org/10.1002/9781118646106.
Hendricks, N.P., Er, E., 2018. Changes in cropland area in the United States and the role of CRP. Food Policy 75, 15–23. https://doi.org/10.1016/J.FOODPOL.2018.02.001.
Hiller, T., Powell, L., McCoy, T., Lusk, J., 2009. Long-term agricultural land-use trends in Nebraska, 1866–2007. Great Plains Res. 19, 225–237.
Isbell, F., Tilman, D., Reich, P.B., Clark, A.T., 2019. Deficits of biodiversity and productivity linger a century after agricultural abandonment. Nat. Ecol. Evol. 3, 1533–1538. https://doi.org/10.1038/s41559-019-1012-1.
Kennedy, R.E., Yang, Z.G., Cohen, W.B., 2010. Detecting trends in forest disturbance and recovery using yearly Landsat time series: 1. LandTrendr – temporal segmentation algorithms. Remote Sens. Environ. 114, 2897–2910. https://doi.org/10.1016/j.rse.2010.07.008.
Ker, A., 1995. Farming Systems of the African Savanna. International Development Research Centre. IDRC.
Khanal, N.R., Watanabe, T., 2009. Abandonment of Agricultural Land and Its Consequences. https://doi.org/10.1659/0276-4741(2006)026[0032:AOALAI]2.0.CO;2https://doi.org/10.1659/0276-4741(2006)026[0032:AOALAI]2.0.CO;2.
Kolecka, N., 2018. Height of successional vegetation indicates moment of agricultural land abandonment. Remote Sens. 10, 1568. https://doi.org/10.3390/rs10101568.
Kuemmerle, T., Hostert, P., Radeloff, V.C., van der Linden, S., Perzanowski, K., Kruhlov, I., 2008. Cross-border comparison of post-socialist farmland abandonment in the Carpathians. Ecosystems 11, 614–628. https://doi.org/10.1007/s10021-008-9146-z.
Laborte, A.G., Maunahan, A.A., Hijmans, R.J., 2010. Spectral signature generalization and expansion can improve the accuracy of satellite image classification. PLoS One 5, e10516. https://doi.org/10.1371/journal.pone.0010516.
Ladikas, M. (Miltos), European Commission. Science, E.and S.U.L..-G. and ethics., European Commission. Science .P.,.P.,.F.,.C.,.P.,.G.,.M.,.L.,.T.,.S.,.V.,.S.O.,.A.,.D.R., S., 2009. Embedding Society in Science & Technology Policy: European and Chinese Perspectives. Office for Official Publications of the European Communities.
Laue, J.E., Arima, E.Y., 2016. Spatially explicit models of land abandonment in the Amazon. J. Land Use Sci. 11, 48–75. https://doi.org/10.1080/1747423X.2014.993341.
Li, S., Li, X., 2017. Global understanding of farmland abandonment: a review and prospects. J. Geogr. Sci. 27, 1123–1150. https://doi.org/10.1007/s11442-017-1426-0.
Li, A., Deng, W., Zhao, W., 2017. Land Cover Change and its Eco- Environmental Responses in Nepal. Springer, Singapore. https://doi.org/10.1007/978-981-10-2890-8_5.
Liu, J., Kuang, W.H., Zhang, Z.X., Xu, X.L., Qin, Y.W., Ning, J., Zhou, W.C., Zhang, S.W., Li, R.D., Yan, C.Z., Wu, S.X., Shi, X.Z., Jiang, N., Yu, D.S., Pan, X.Z., Chi, W.F., 2014. Spatiotemporal characteristics, patterns, and causes of land-use changes in China since the late 1980s. J. Geogr. Sci. 24, 195–210. https://doi.org/10.1007/s11442-014-1082-6.
Löw, F., Fliemann, E., Abdullaev, I., Conrad, C., Lamers, J.P.A., 2015. Mapping abandoned agricultural land in Kyzyl-Orda, Kazakhstan using satellite remote sensing. Appl. Geogr. 62, 377–390. https://doi.org/10.1016/J.APGEOG.2015.05.009.
Lü, Y., Fu, B., Feng, X., Zeng, Y., Liu, Y., Chang, R., Sun, G., Wu, B., 2012. A policy-driven large scale ecological restoration: quantifying ecosystem services changes in the loess plateau of China. PLoS One 7, e31782. https://doi.org/10.1371/journal.pone.0031782.
MacDonald, D., Crabtree, J.R., Wiesinger, G., Dax, T., Stamou, N., Fleury, P., Gutierrez Lazpita, J., Gibon, A., 2000. Agricultural abandonment in mountain areas of Europe: environmental consequences and policy response. J. Environ. Manag. https://doi.org/10.1006/jema.1999.0335.
Masek, J.G., Vermote, E.F., Saleous, N.E., Wolfe, R., Hall, F.G., Huemmrich, K.F., Gao, F., Kutler, J., Lim, T.-K., 2006. A Landsat surface reflectance dataset for North America, 1990–2000. IEEE Geosci. Remote Sens. Lett. 3, 68–72. https://doi.org/10.1109/LGRS.2005.857030.
Miller, D.C., Muñoz-Mora, J.C., Christiaensen, L., 2017. Prevalence, economic contribution, and determinants of trees on farms across Sub-Saharan Africa. For. Policy Econ. https://doi.org/10.1016/j.forpol.2016.12.005.
Monfreda, C., Ramankutty, N., Foley, J.A., 2008. Farming the planet: 2. Geographic distribution of crop areas, yields, physiological types, and net primary production in the year 2000. Glob. Biogeochem. Cycles 22. https://doi.org/10.1029/2007GB002947.
Mottet, A., Ladet, S., Coqué, N., Gibon, A., 2006. Agricultural land-use change and its drivers in mountain landscapes: a case study in the Pyrenees. Agric. Ecosyst. Environ. https://doi.org/10.1016/j.agee.2005.11.017.
Mueller, H., Rufin, P., Griffiths, P., Siqueira, A.J.B., Hostert, P., 2015. Mining dense Landsat time series for separating cropland and pasture in a heterogeneous Brazilian savanna landscape. Remote Sens. Environ. 156, 490–499. https://doi.org/10.1016/j.rse.2014.10.014.
Munroe, D.K., van Berkel, D.B., Verburg, P.H., Olson, J.L., 2013. Alternative trajectories of land abandonment: causes, consequences and research challenges. Curr. Opin. Environ. Sustain. https://doi.org/10.1016/j.cosust.2013.06.010.
Nguyen, H., Hölzel, N., Völker, A., Kamp, J., Nguyen, H., Hölzel, N., Völker, A., Kamp, J., 2018. Patterns and determinants of post-soviet cropland abandonment in the Western Siberian Grain Belt. Remote Sens. 10, 1973. https://doi.org/10.3390/rs10121973.
O'Hara, S.L., 1997. Irrigation and land degradation: implications for agriculture in Turkmenistan, Central Asia. J. Arid Environ. https://doi.org/10.1006/jare.1996.0238.
Olofsson, P., Foody, G.M., Herold, M., Stehman, S.V., Woodcock, C.E., Wulder, M.A., 2014. Good practices for estimating area and assessing accuracy of land change. Remote Sens. Environ. 148, 42–57. https://doi.org/10.1016/j.rse.2014.02.015.
Olthof, I., Butson, C., Fraser, R., 2005. Signature extension through space for northern landcover classification: a comparison of radiometric correction methods. Remote Sens. Environ. https://doi.org/10.1016/j.rse.2004.12.015.
Osawa, T., Kohyama, K., Mitsuhashi, H., 2016. Multiple factors drive regional agricultural abandonment. Sci. Total Environ. https://doi.org/10.1016/j.scitotenv.2015.10.067.
Ozdogan, M., Woodcock, C.E., 2006. Resolution dependent errors in remote sensing of cultivated areas. Remote Sens. Environ. 103, 203–217. https://doi.org/10.1016/j.rse.2006.04.004.
Parés-Ramos, I.K., Gould, W.A., Aide, T.M., 2008. Agricultural abandonment, suburban growth, and forest expansion in Puerto Rico between 1991 and 2000. Ecol. Soc. https://doi.org/10.5751/ES-02479-130201.
Pax-Lenney, M., Woodcock, C.E., Macomber, S.A., Gopal, S., Song, C., 2001. Forest mapping with a generalized classifier and Landsat TM data. Remote Sens. Environ. 77, 241–250. https://doi.org/10.1016/S0034-4257(01)00208-5.
Pekel, J.-F., Cottam, A., Gorelick, N., Belward, A.S., 2016. High-resolution mapping of global surface water and its long-term changes. Nature. https://doi.org/10.1038/nature20584.
Pesaresi, M., Ehrlich, D., Florczyk, A., Freire, S., Julea, A., Kemper, T., Soille, P., Syrris, V., 2015. GHS built-up grid, derived from Landsat, multitemporal (1975, 1990, 2000, 2014). In: European Commission, Joint Research Centre (JRC) [Dataset] PID, . http://data.europa.eu/89h/jrc-ghsl-ghs_built_ldsmt_globe_r2015b.
Pflugmacher, D., Rabe, A., Peters, M., Hostert, P., 2019. Mapping pan-European land cover using Landsat spectral-temporal metrics and the European LUCAS survey. Remote Sens. Environ. 221, 583–595. https://doi.org/10.1016/J.RSE.2018.12.001.
Pinto Correia, T., 1993. Land abandonment: changes in the land use patterns around the Mediterranean basin. In: Etat de l'Agriculture En Méditerranée. Les Sols Dans La Région Méditerranéenne. Utilisation, Gestion et Perspectives d'évolution.
Poeplau, C., Don, A., Vesterdal, L., Leifeld, J., Van Wesemael, B., Schumacher, Je, Gensior, A., 2011. Temporal dynamics of soil organic carbon after land-use change in the temperate zone –- carbon response functions as a model approach. Glob. Chang. Biol. 17, 2415–2427. https://doi.org/10.1111/j.1365-2486.2011.02408.x.
Pointereau, P., Coulon, F.P., Girard, M.L., Stuczynski, T., Ortega, V.S., Del Rio, A., 2008. Analysis of farmland abandonment and the extent and location of agricultural areas that are actually abandoned or are in risk to be abandoned. In: Anguiano, E., Bamps, C., Terres, J.-M. (Eds.), JRC Scientific and Technical Reports (EUR 23411 EN).
Porwollik, V., Rolinski, S., Heinke, J., Müller, C., 2019. Generating a rule-based global gridded tillage dataset. Earth Syst. Sci. Data 11, 823–843. https://doi.org/10.5194/essd-11-823-2019.
Potapov, P.V., Turubanova, S.A., Hansen, M.C., Adusei, B., Broich, M., Altstatt, A., Mane, L., Justice, C.O., 2012. Quantifying forest cover loss in Democratic Republic of the Congo, 2000–2010, with Landsat ETM+ data. Remote Sens. Environ. 122, 106–116. https://doi.org/10.1016/j.rse.2011.08.027.
Potapov, P.V., Turubanova, S.A., Tyukavina, A., Krylov, A.M., McCarty, J.L., Radeloff, V.C., Hansen, M.C., 2015. Eastern Europe's forest cover dynamics from 1985 to 2012 quantified from the full Landsat archive. Remote Sens. Environ. https://doi.org/10.1016/j.rse.2014.11.027.
Powers, D.M.W., 2011. Evaluation: from precision, recall and f-measure to roc, informedness, markedness and correlation. J. Mach. Learn. Technol. 2, 37–63.

Prishchepov, A.V., Radeloff, V.C., Baumann, M., Kuemmerle, T., Müller, D., 2012. Effects of institutional changes on land use: agricultural land abandonment during the transition from state-command to market-driven economies in post-Soviet Eastern Europe. Environ. Res. Lett. 7, 024021. https://doi.org/10.1088/1748-9326/7/2/024021.

Prishchepov, A.A., Müller, D., Dubinin, M., Baumann, M., Radeloff, V.C., 2013. Determinants of agricultural land abandonment in post-Soviet European Russia. Land Use Policy 30, 873–884. https://doi.org/10.1016/j.landusepol.2012.06.011.

Queiroz, C., Beilin, R., Folke, C., Lindborg, R., 2014. Farmland abandonment: threat or opportunity for biodiversity conservation? A global review. Front. Ecol. Environ. https://doi.org/10.1890/120348.

Ramankutty, N., Foley, J.A., 1999. Estimating historical changes in land cover:north American croplands from 1850 to 1992. GCTE/LUCC RESEARCH ARTICLE. Glob. Ecol. Biogeogr. 8 (5), 381–396. https://doi.org/10.1046/j.1365-2699.1999.00141.x.

Rikimaru, A., Roy, P.S., Miyatake, S., 2002. Tropical forest cover density mapping. Trop. Ecol. 43, 39–47.

Roy, D.P., Kovalskyy, V., Zhang, H.K., Vermote, E.F., Yan, L., Kumar, S.S., Egorov, A., 2016. Characterization of Landsat-7 to Landsat-8 reflective wavelength and normalized difference vegetation index continuity. Remote Sens. Environ. 185, 57–70. https://doi.org/10.1016/J.RSE.2015.12.024.

Ruskule, A., Nikodemus, O., Kasparinska, Z., Kasparinskis, R., Brūmelis, G., 2012. Patterns of afforestation on abandoned agriculture land in Latvia. Agrofor. Syst. https://doi.org/10.1007/s10457-012-9495-7.

Shoyama, K., Braimoh, A.K., 2011. Analyzing about sixty years of land-cover change and associated landscape fragmentation in Shiretoko Peninsula, Northern Japan. Landsc. Urban Plan. https://doi.org/10.1016/j.landurbplan.2010.12.016.

Su, G., Okahashi, H., Chen, L., Su, G., Okahashi, H., Chen, L., 2018. Spatial pattern of farmland abandonment in Japan: identification and determinants. Sustainability 10, 3676. https://doi.org/10.3390/su10103676.

Thenkabail, P.S., Knox, J.W., Ozdogan, M., Gumma, M.K., Congalton, R.G., ZHUOTING, W.U., Milesi, C., Finkral, A., Marshall, M., Mariotto, I., 2012. Assessing future risks to agricultural productivity, water resources and food security: how can remote sensing help? Photogramm. Eng. Remote. Sens. 78 (8), 773–782.

USDA NASS, 2018. USDA, National Agricultural Statistics Service, Cultivated Layer. USDA, NASS Marketing and Information Services Office, Washington, D.C.

Verbesselt, J., Hyndman, R., Newnham, G., Culvenor, D., 2010. Detecting trend and seasonal changes in satellite image time series. Remote Sens. Environ. 114, 106–115. https://doi.org/10.1016/j.rse.2009.08.014.

Vermote, E., Justice, C., Claverie, M., Franch, B., 2016. Preliminary analysis of the performance of the Landsat 8/OLI land surface reflectance product. Remote Sens. Environ. 185, 46–56. https://doi.org/10.1016/j.rse.2016.04.008.

Vicente-Serrano, S.M., Pérez-Cabello, F., Lasanta, T., 2008. Assessment of radiometric correction techniques in analyzing vegetation variability and change using time series of Landsat images. Remote Sens. Environ. 112, 3916–3934. https://doi.org/10.1016/j.rse.2008.06.011.

Vuichard, N., Ciais, P., Belelli, L., Smith, P., Valentini, R., 2008. Carbon sequestration due to the abandonment of agriculture in the former USSR since 1990. Glob. Biogeochem. Cycles 22. https://doi.org/10.1029/2008GB003212.

Walther, P., 1986. Land abandonment in the Swiss Alps: a new understanding of a land-use problem. Mt. Res. Dev. 6, 305. https://doi.org/10.2307/3673371.

Wang, C., Gao, Q., Wang, X., Yu, M., 2015. Decadal trend in agricultural abandonment and woodland expansion in an agro-pastoral transition band in northern China. PLoS One 10, e0142113. https://doi.org/10.1371/journal.pone.0142113.

Wertebach, T.-M., Hölzel, N., Kämpf, I., Yurtaev, A., Tupitsin, S., Kiehl, K., Kamp, J., Kleinebecker, T., 2017. Soil carbon sequestration due to post-Soviet cropland abandonment: estimates from a large-scale soil organic carbon field inventory. Glob. Chang. Biol. 23, 3729–3741. https://doi.org/10.1111/gcb.13650.

Wickham, J.D., Stehman, S.V., Gass, L., Dewitz, J., Fry, J.A., Wade, T.G., 2013. Accuracy assessment of NLCD 2006 land cover and impervious surface. Remote Sens. Environ. 130, 294–304.

Witmer, F.D.W., 2008. Detecting war-induced abandoned agricultural land in northeast Bosnia using multispectral, multitemporal Landsat TM imagery. Int. J. Remote Sens. 29, 3805–3831. https://doi.org/10.1080/01431160801891879.

Woodcock, C.E., Macomber, S.A., Pax-Lenney, M., Cohen, W.B., 2001. Monitoring large areas for forest change using Landsat: generalization across space, time and Landsat sensors. Remote Sens. Environ. 78, 194–203. https://doi.org/10.1016/S0034-4257(01)00259-0.

Xu, Y., Yu, L., Zhao, F.R., Cai, X., Zhao, J., Lu, H., Gong, P., 2018. Tracking annual cropland changes from 1984 to 2016 using time-series Landsat images with a change-detection and post-classification approach: experiments from three sites in Africa. Remote Sens. Environ. 218, 13–31. https://doi.org/10.1016/J.RSE.2018.09.008.

Yan, J., Yang, Z., Li, Z., Li, X., Xin, L., Sun, L., 2016. Drivers of cropland abandonment in mountainous areas: a household decision model on farming scale in Southwest China. Land Use Policy 57, 459–469. https://doi.org/10.1016/j.landusepol.2016.06.014.

Yin, H., Khamzina, A., Pflugmacher, D., Martius, C., 2017. Forest cover mapping in post-Soviet Central Asia using multi-resolution remote sensing imagery. Sci. Rep. 7, 1375.

Yin, H., Pflugmacher, D., Li, A., Li, Z., Hostert, P., 2018a. Land use and land cover change in Inner Mongolia – understanding the effects of China's re-vegetation programs. Remote Sens. Environ. 204, 918–930. https://doi.org/10.1016/J.RSE.2017.08.030.

Yin, H., Prishchepov, A.V., Kuemmerle, T., Bleyhl, B., Buchner, J., Radeloff, V.C., 2018b. Mapping agricultural land abandonment from spatial and temporal segmentation of Landsat time series. Remote Sens. Environ. 210, 12–24. https://doi.org/10.1016/j.rse.2018.02.050.

Yin, H., Butsic, V., Buchner, J., Kuemmerle, T., Prishchepov, A.V., Baumann, M., Bragina, E.V., Sayadyan, H., Radeloff, V.C., 2019. Agricultural abandonment and re-cultivation during and after the Chechen Wars in the northern Caucasus. Glob. Environ. Chang. 55, 149–159. https://doi.org/10.1016/J.GLOENVCHA.2019.01.005.

Yusoff, N., Muharam, F., Yusoff, N.M., Muharam, F.M., 2015. The use of multi-temporal Landsat imageries in detecting seasonal crop abandonment. Remote Sens. 7, 11974–11991. https://doi.org/10.3390/rs70911974.

Zhang, Bailin, Yang, Q., Yan, Y., Xue, M., Su, K., Zhang, Bo, 2011. Characteristics and reasons of different households' farming abandonment behavior in the process of rapid urbanization based on a survey from 540 households in 10 counties of Chongqing municipality. Resour. Sci. 33, 2047–2054.

Zhou, D.C., Zhao, S.Q., Zhu, C., 2012. The grain for Green project induced land cover change in the loess plateau: a case study with Ansai County, Shanxi Province, China. Ecol. Indic. 23, 88–94. https://doi.org/10.1016/j.ecolind.2012.03.021.

Zhu, Z., Woodcock, C.E., 2014. Continuous change detection and classification of land cover using all available Landsat data. Remote Sens. Environ. 144, 152–171. https://doi.org/10.1016/j.rse.2014.01.011.